Chapter 9

# Multiwavelength Digital Holography and Phase-Shifting Interferometry Selectively Extracting Wavelength Information: Phase-Division Multiplexing (PDM) of Wavelengths

Tatsuki Tahara, Reo Otani, Yasuhiko Arai and Yasuhiro Takaki

Additional information is available at the end of the chapter

http://dx.doi.org/10.5772/67295

**Abstract**

In this chapter, we introduce multiwavelength digital holographic techniques and a novel multiwavelength imaging technique. General multiwavelength imaging systems adopt temporal division, spatial division, or space-division multiplexing to obtain wavelength information. Holographic techniques give us unique multiwavelength imaging systems, which utilize temporal or spatial frequency-division multiplexing. Conventional multiwavelength digital holography systems have been combined with one of the methods listed above. We have proposed phase-shifting interferometry selectively extracting wavelength information, characterized as a multiwavelength three-dimensional (3D) imaging technique based on holography and called phase-division multiplexing (PDM) of multiple wavelengths. In PDM, wavelength-multiplexed phase-shifted holograms are recorded, and multiwavelength information is separately extracted from the holograms in the space domain. Phase shifts are introduced for respective wavelengths to separate object waves with multiple wavelengths in the polar coordinate plane, and multiple object waves are selectively extracted by the signal processing based on phase-shifting interferometry. Additionally, the system of equations needed to obtain a multiwavelength 3D image is solved with less wavelength-multiplexed images using two-step phase-shifting interferometry-merged phase-division multiplexing ($2\pi$-PDM), which makes the best use of $2\pi$ ambiguity of the phase and two-step phase-shifting method. The PDM techniques are reviewed and color 3D imaging ability is described with numerical and experimental results.

**Keywords:** digital holography, holography, interferometry, holographic interferometry, phase-shifting interferometry, multiwavelength interferometry, color holography, multiwavelength 3D imaging, color 3D imaging, multiwavelength imaging, phase-division multiplexing of wavelengths, $2\pi$-PDM

## 1. Introduction

Holography [1–4] is a technique to record a wavefront of an object wave by utilizing interference of light as well as reconstruct a three-dimensional (3D) image of an object. The medium containing the information of an interference fringe image is called a "hologram", which contains both the amplitude and phase information of an object wave. 3D image information is reconstructed using a hologram and diffraction theory. One of the most remarkable features in holography is that 3D motion-picture recording of any ultrafast physical phenomenon can be achieved, even for light propagation in 3D space [3]. Digital holography [5–8] is a technique to record a hologram digitally using an image sensor, and reconstruct both the 3D and quantitative phase images of an object using a computer or spatial light modulator. This technique has been researched for not only the observation of ultrafast phenomenon, but also for microscopy [9, 10], quantitative phase imaging [11, 12], and multimodal imaging [13, 14].

In recent years, there has been an increase in demand for multispectral imaging techniques. Multiwavelength information helps us to perceive, analyze, and recognize an object such as body tissue or a tumor. Wavelength of light has the ability to clarify color and material distributions of an object [15], visualize the localization and dynamics of molecules with Raman scattering [16, 17], and analyze the health of human skin [18]. In digital holography, the information of multiple wavelengths and 3D space is obtained by recording waves with multiple wavelengths that are irradiated from light sources, called multiwavelength/color digital holography [19, 20]. Multiwavelength digital holography has the ability for not only color 3D imaging [19, 20], but also dispersion imaging [21] and 3D shape measurement with a wide range by using multiwavelength phase unwrapping [22], due to the recording of quantitative phase information with multiple wavelengths. Temporal division [23–25], spatial division [26–28], and space-division multiplexing [19, 20, 29], which are generally adopted for multiwavelength imaging in an imaging system, can be merged into digital holography to record multiple wavelengths. In general imaging systems, wavelength information is temporally or spatially separated when recording image(s), as shown in **Figure 1(a)–(e)**. However, holographic techniques make it possible to record multiwavelength/color information using a monochromatic image sensor and to reconstruct it from wavelength-multiplexed image(s). In holography, multiple wavelength information is obtained also by utilizing temporal frequency-division multiplexing (**Figure 1(f)**) [30, 31] and spatial frequency-division multiplexing (**Figure 1(g)**) [32, 33]. In these techniques, Fourier and inverse Fourier transforms are required to separate wavelength information. In the former, many wavelength-multiplexed images and an image sensor with a high frame rate are needed. In the latter, the spatial bandwidth available for recording an object wave at a wavelength is restricted as the number of wavelengths is increased.

Since 2013, we have presented a novel multiwavelength imaging technique utilizing holography and wavelength-multiplexed images [34–39]. The presented technique gives phase-shifting interferometry [40–51] the function to extract wavelength information such as wavelength dependencies of amplitude, phase, and polarization state selectively from wavelength-multiplexed phase-shifted holograms. It is especially important to record not only phase images but also amplitude distributions of object waves at multiple wavelengths in order to achieve multicolor and multispectral 3D imaging of multiple objects. By making use of holography for multiwavelength imaging, 3D space information is simultaneously captured. In this

http://dx.doi.org/10.5772/67295

chapter, we explain the proposed technique, phase-shifting interferometry selectively extracting wavelength information: phase-division multiplexing (PDM) of multiple wavelengths and two-step phase-shifting interferometry-merged phase-division multiplexing (2π-PDM).

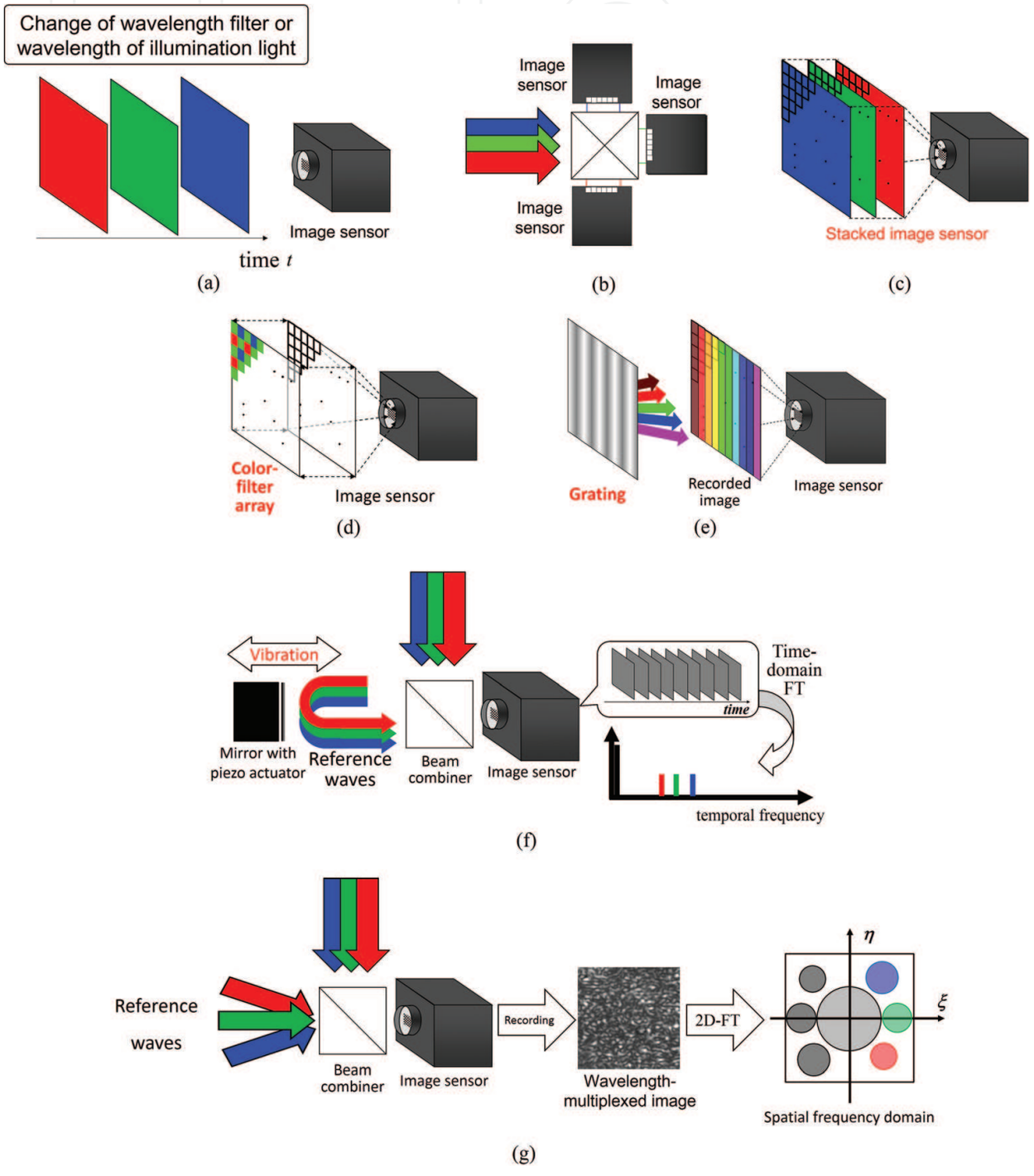


**Figure 1.** Multiwavelength imaging systems. (a) Temporal division, spatial division with (b) multiple image sensors and a prism and (c) a stacked image sensor, space-division multiplexing with (d) a color image sensor and (e) a grating, (f) temporal frequency-division multiplexing, and (g) spatial frequency-division multiplexing.

## 2. Phase-shifting interferometry selectively extracting wavelength information: phase-division multiplexing (PDM) of wavelengths

**Figure 2** illustrates the schematic of the proposed multiwavelength 3D imaging technique in the case where the number of wavelengths $N$ is two, which was initially presented in 2013 [34–36]. Optical setup is based on phase-shifting digital holography with multiple lasers. Multiple object and reference waves with multiple wavelengths illuminate a monochromatic image sensor simultaneously. The sensor records wavelength-multiplexed phase-shifted holograms $I(x,y:\alpha_1,\alpha_2)$ by changing the phases of the reference waves. Phase shifts for respective wavelengths $\alpha_1$ and $\alpha_2$ are introduced. An object wave at the desired wavelength is selectively extracted from the holograms by the signal processing based on phase-shifting interferometry. As a result, a color 3D image is reconstructed from the selectively extracted object waves. Thus, color 3D imaging can be achieved with grayscale wavelength-multiplexed images. When the number of wavelengths is $N$, $2N + 1$ variables are contained in a wavelength-multiplexed hologram: the number $N$ of object waves, $N$ of conjugate images, and the sum of the 0th-order diffraction waves. Therefore, five holograms are required to solve the system of equations when $N = 2$. It is noted that no Fourier transform is essentially required.

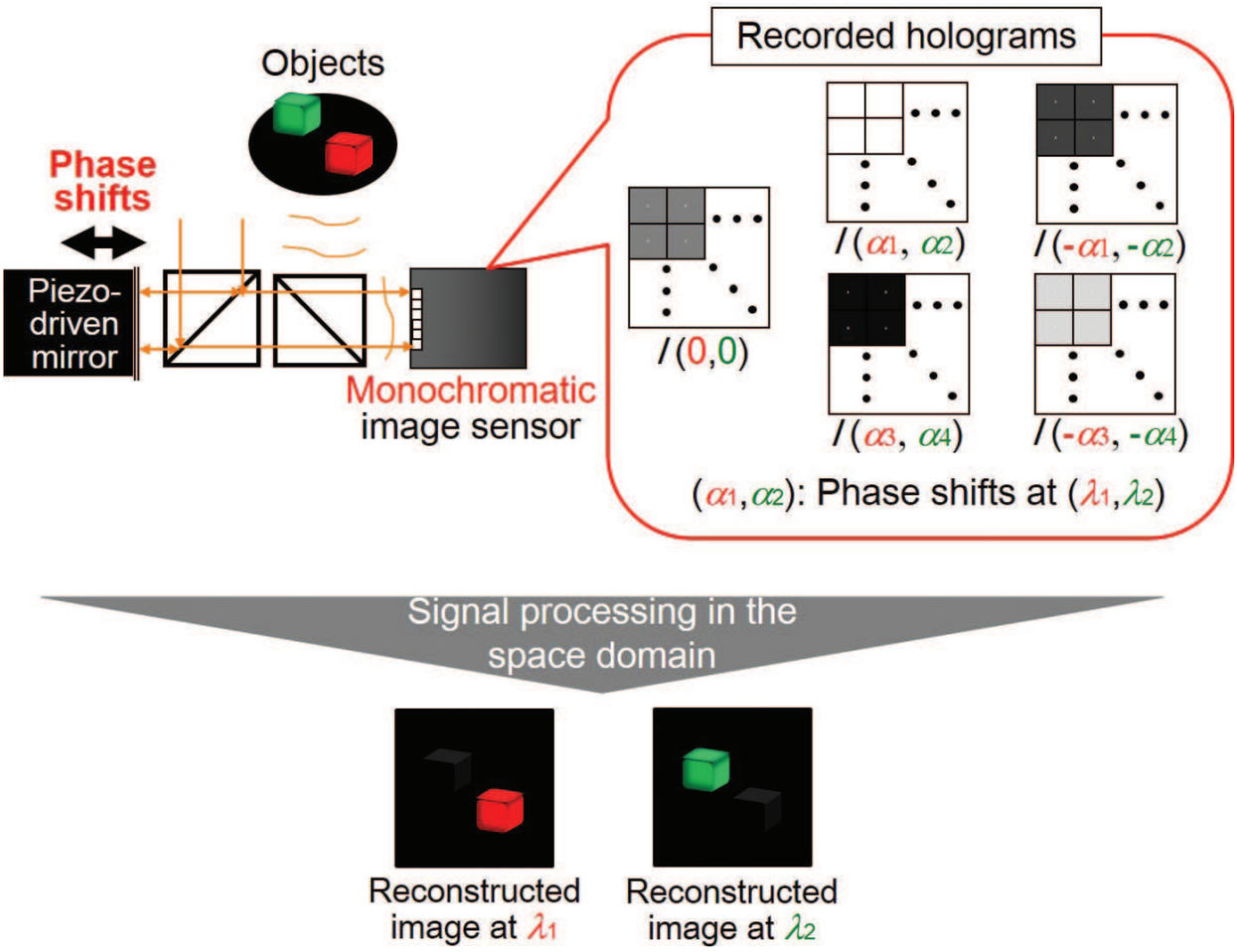


**Figure 2.** Schematic representation of the proposed multiwavelength 3D imaging technique.

http://dx.doi.org/10.5772/67295

**Figure 3** describes the principle that wavelength information is selectively extracted by the signal processing in the space domain. As seen in **Figure 3**, different phase shifts for respective wavelengths are given to object waves with multiple wavelengths, and then wavelength information is separated in the polar coordinate plane. Although this separation is used to extract an object wave from a hologram in general phase-shifting interferometry, in the proposed technique, the separation is utilized to remove not only the conjugate images and 0th-order diffraction wave, but also undesired wavelength information. This means phase-division multiplexing (PDM) of wavelengths. **Figure 3** shows the case where specific phase shifts are used [34–36], but this concept is also applicable to the case where arbitrary phase shifts are introduced [39].

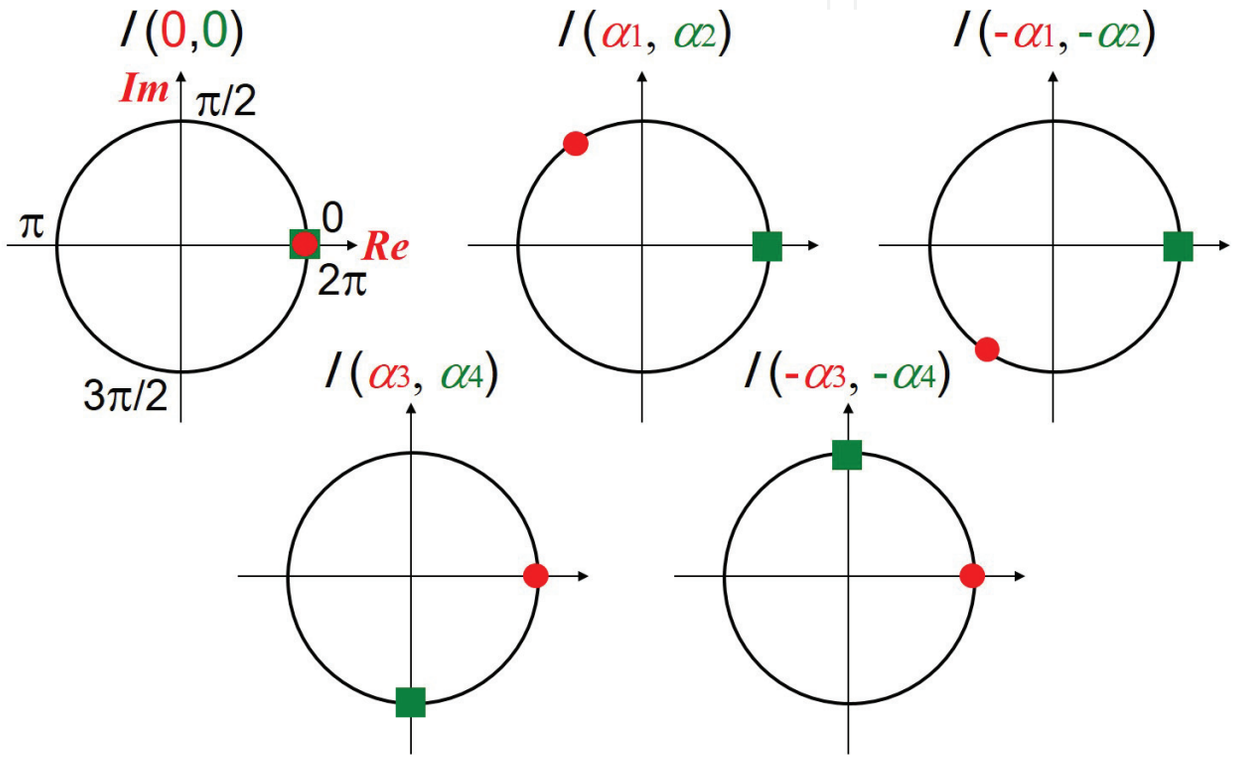


**Figure 3.** Principle of phase-division multiplexing (PDM) of wavelengths: separation of multiple wavelengths in the polar coordinate plane.

**Figure 4** illustrates optical implementations of the proposed digital holography. Multiple lasers irradiate laser beams with multiple wavelengths simultaneously. A device for shifting the phase of light, such as a mirror with a piezo actuator, a spatial light modulator, or wave plates, is placed in the path of the reference arm. A monochromatic image sensor records the required wavelength-multiplexed phase-shifted holograms sequentially. An optical system based on PDM has the following features: the spectroscopic sensitivity of the optical system can be extended in comparison to the system with a color image sensor; full space-bandwidth product of an image sensor can be used to record object waves with multiple wavelengths; a bright color image can be obtained due to no spectroscopic absorption, while wavelengths filters required in conventional systems absorb light to obtain a color image; and measurement time is shortened by the wavelength-multiplexed recording in comparison with temporal division technique.

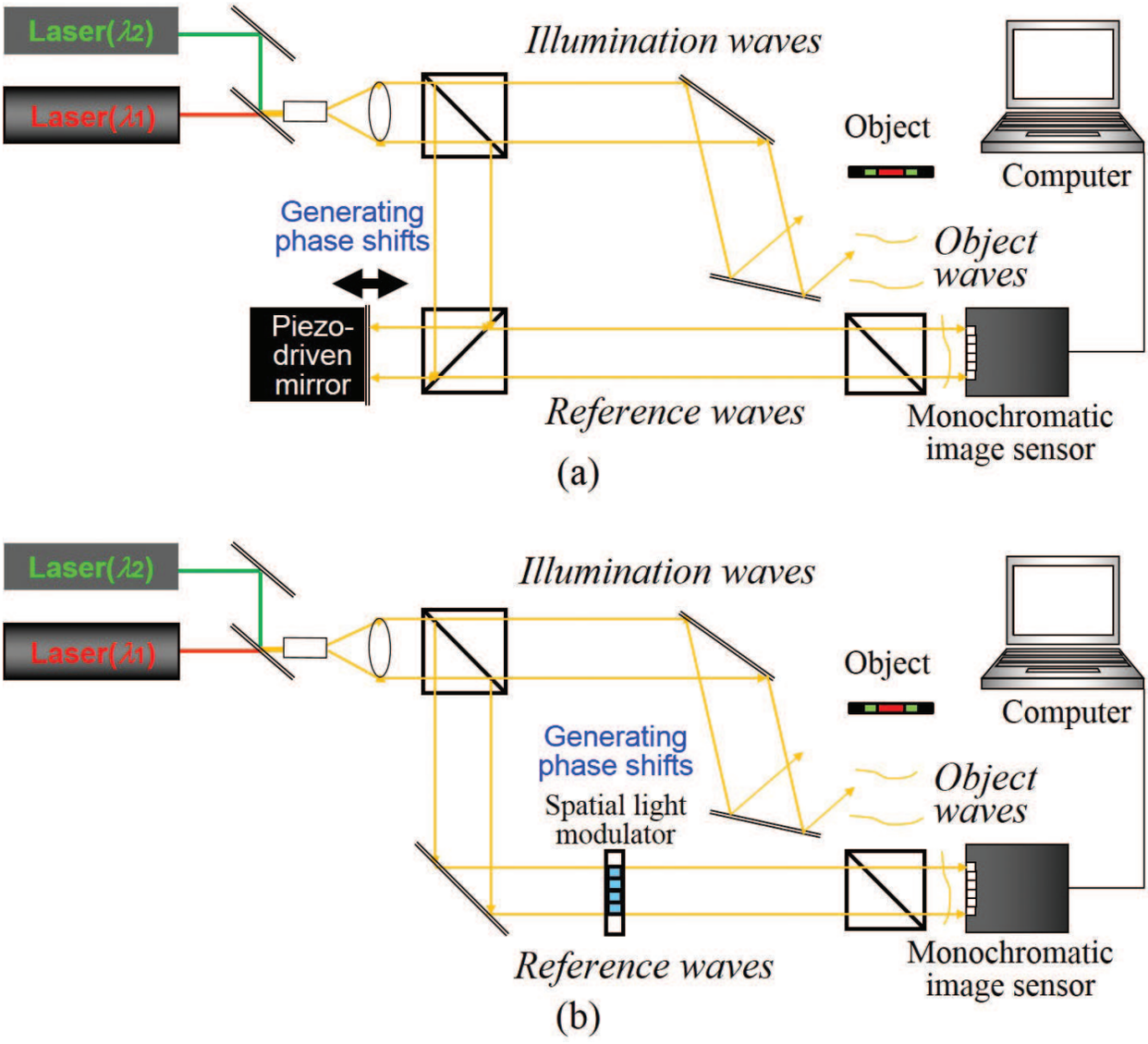


**Figure 4.** Optical implementations of PDM. Optical setups with (a) a mirror with a piezo actuator and (b) a spatial light modulator that has wavelength dependency in phase modulation.

**Figure 5** illustrates the image reconstruction algorithm [34–36]. A wavelength-multiplexed phase-shifted hologram $I(x,y{:}\alpha_1,\alpha_2)$ is expressed as follows,

$$I(x,y:\alpha_1,\alpha_2) = I_{\lambda 1}(x,y:\alpha_1) + I_{\lambda 2}(x,y:\alpha_2), \tag{1}$$

here $I_{\lambda 1}(x,y{:}\alpha_1)$ and $I_{\lambda 2}(x,y{:}\alpha_2)$ are holograms at the wavelengths of $\lambda_1$ and $\lambda_2$, respectively. Eq. (1) means that a recorded monochromatic image is the sum of $I_{\lambda 1}(x,y{:}\alpha_1)$ and $I_{\lambda 2}(x,y{:}\alpha_2)$. When the complex amplitude distributions of object waves with different wavelengths are $U_{\lambda 1}(x,y)$ and $U_{\lambda 2}(x,y)$, $0th(x,y)$ is the 0th-diffraction wave, $Ar(x,y)$ is the amplitude distribution of the reference wave, $j$ is imaginary unit, $^*$ means complex conjugate, and $L$ and $M$ are integers, then $I(x,y{:}\alpha_1,\alpha_2)$ can be rewritten as follows,

http://dx.doi.org/10.5772/67295

$$I(x,y:\alpha_1,\alpha_2) = 0th_{\lambda 1}(x,y) + Ar_{\lambda 1}(x,y)\{U_{\lambda 1}(x,y)\exp(-j\alpha_1) + U_{\lambda 1}{}^{*}(x,y)\exp(j\alpha_1)\} + 0th_{\lambda 2}(x,y) + Ar_{\lambda 2}(x,y)\{U_{\lambda 2}(x,y)\exp(-j\alpha_2) + U_{\lambda 2}{}^{*}(x,y)\exp(j\alpha_2)\}. \quad (2)$$

Only the complex amplitude distributions of object waves with dual wavelengths $U_{\lambda 1}(x,y)$ and $U_{\lambda 2}(x,y)$ are derived from five wavelength-multiplexed phase-shifted holograms $I(x,y:0,0)$, $I(x,y:\alpha_1,\alpha_2)$, $I(x,y:-\alpha_1,-\alpha_2)$, $I(x,y:\alpha_3,\alpha_4)$, and $I(x,y:-\alpha_3,-\alpha_4)$ because five variables are contained in Eq. (2). If the system shown in **Figure 4(a)** is used to implement the proposed technique by moving the mirror in the reference arm with a piezo actuator at a distance $Z$ in the depth direction, the phase shifts are

$$\alpha_1 = \frac{4\pi Z}{\lambda_1}, \quad (3)$$

$$\alpha_2 = \frac{4\pi Z}{\lambda_2}. \quad (4)$$

Here, when $Z$ is equal to $L\lambda_1/2$, $\alpha_1$ is $2\pi L$ and $\alpha_2$ is $2\pi L\lambda_1/\lambda_2$. As a result, the intensity distribution $I_{\lambda 1}(x,y:\alpha_1)$ is not changed and $I_{\lambda 2}(x,y:\alpha_2)$ is changed, unless $L\lambda_1/\lambda_2$ is an integer. In the case where an integral multiple of $2\pi$ is utilized for phase shifts, meaning $\alpha_2 = 2\pi M$ and $\alpha_3 = 2\pi L$, $U_{\lambda 1}(x,y)$ and $U_{\lambda 2}(x,y)$ are separately derived by the following expressions.

$$U_{\lambda 1}(x,y) = [2I(x,y:0,0) - \{I(x,y:\alpha_1,2\pi M) + I(x,y:-\alpha_1,-2\pi M)\}]/\{4Ar_{\lambda 1}(x,y)(1-\cos\alpha_1)\} + j\{I(x,y:-\alpha_1,-2\pi M) - I(x,y:\alpha_1,2\pi M)\}/(4Ar_{\lambda 1}(x,y)\sin\alpha_1), \quad (5)$$

$$U_{\lambda 2}(x,y) = [2I(x,y:0,0) - \{I(x,y:2\pi L,\alpha_4) + I(x,y:-2\pi L,-\alpha_4)\}]/\{4Ar_{\lambda 2}(x,y)(1-\cos\alpha_4)\} + j\{I(x,y:-2\pi L,-\alpha_4) - I(x,y:2\pi L,\alpha_4)\}/(4Ar_{\lambda 2}(x,y)\sin\alpha_4). \quad (6)$$

As shown in Eqs. (5) and (6), subtraction between holograms, which is based on phase-shifting interferometry, is calculated and the unwanted wavelength component $I_{\lambda 1}(x,y)$ or $I_{\lambda 2}(x,y)$ is removed. Thus, dual-wavelength information is extracted selectively from five phase-shifted holograms. In this way, multiwavelength information can be separately extracted from $2N + 1$ holograms when the number of wavelengths is $N$. From the extracted complex amplitude distributions on the image sensor plane, a multiwavelength 3D object image is reconstructed by the calculations of diffraction integrals and color synthesis.

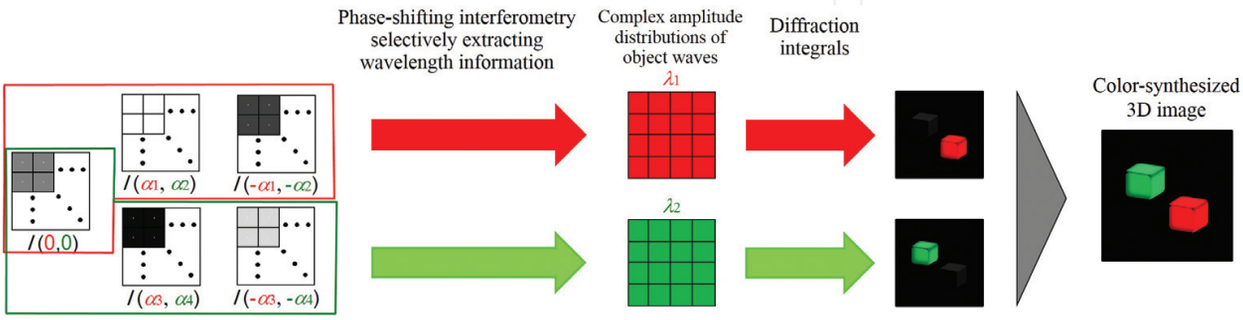


**Figure 5.** Image-reconstruction procedure.

## 3. Numerical simulation

Numerical simulations were conducted to verify the effectiveness of the proposed technique. **Figure 6** shows the amplitude and phase distributions of the object wave at each wavelength. As shown in **Figure 6(b)**, a color object with rough surface was assumed. 640 and 532 nm were assumed as the wavelengths of the light sources. Red and green color components of a standard image "pepper" were used as amplitude images at 640 and 532 nm, respectively. In these simulations, the distance between the object and image sensor was assumed as 200 mm, pixel pitch was 5 μm, resolution was 10 bits, and number of pixels was 512 × 512. **Figure 7** shows the images reconstructed by the proposed technique. Faithful images were reconstructed at each wavelength, and crosstalk between object waves with different wavelengths was not seen. The color synthesized image in **Figure 7(c)** indicates color 3D imaging ability. Thus, the validity of the proposed technique was numerically confirmed. Detailed numerical analyses and an experimental demonstration using an image sensor with 12-bit resolution were reported in Ref. [36].

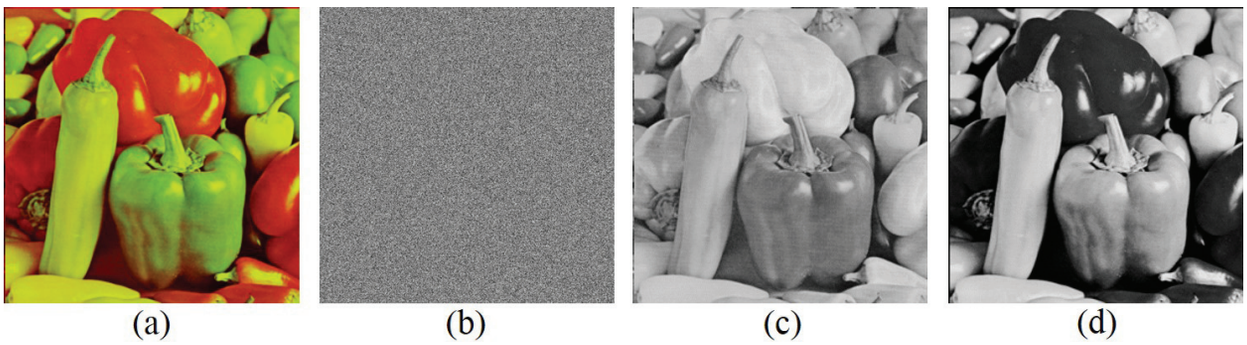


**Figure 6.** Object wave for a numerical simulation. (a) Amplitude and (b) phase distributions of the object wave. Assumed amplitude images at the wavelengths of (c) 640 nm and (d) 532 nm.

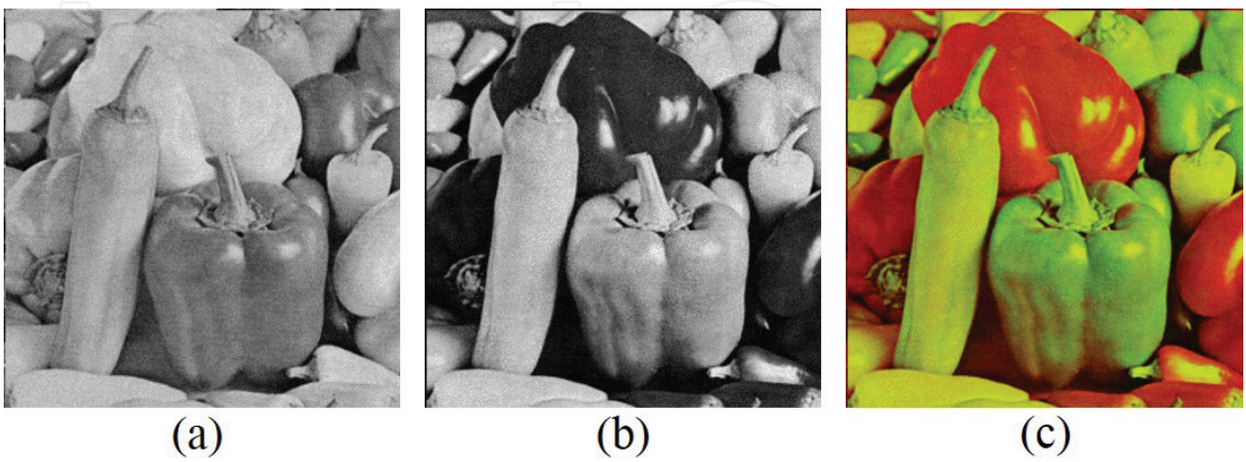


**Figure 7.** Numerical results. Reconstructed images at the wavelengths of (a) 640 nm and (b) 532 nm. (c) Color synthesized image.

http://dx.doi.org/10.5772/67295

## 4. Two-step phase-shifting interferometry-merged phase-division multiplexing (2π-PDM)

In a wavelength-multiplexed hologram, $2N + 1$ variables are contained. Therefore, $2N + 1$ images are needed to extract object waves separately in a general PDM technique. However, $2N$ wavelength-multiplexed holograms are sufficient to selectively extract object waves with $N$ wavelengths, with the two-step phase-shifting interferometry-merged phase-division multiplexing (2π-PDM) technique [38]. **Figure 8** illustrates the basic concept of 2π-PDM. Two main points of 2π-PDM are the utilization of 2π ambiguity of the phase [34, 35] and merger of two-step phase-shifting interferometry [52–56]. As described in section 2, an intensity distribution at a wavelength is not changed when a phase shift is an integral multiple of 2π. We make the best use of this nature to decrease the required number of wavelength-multiplexed images. Also, merging PDM and two-step phase-shifting interferometry is important to satisfy high-quality multiwavelength 3D imaging and acceleration of a recording simultaneously. When recording three wavelengths, six holograms are sufficient with 2π-PDM, as described with an optical implementation in Ref. [38].

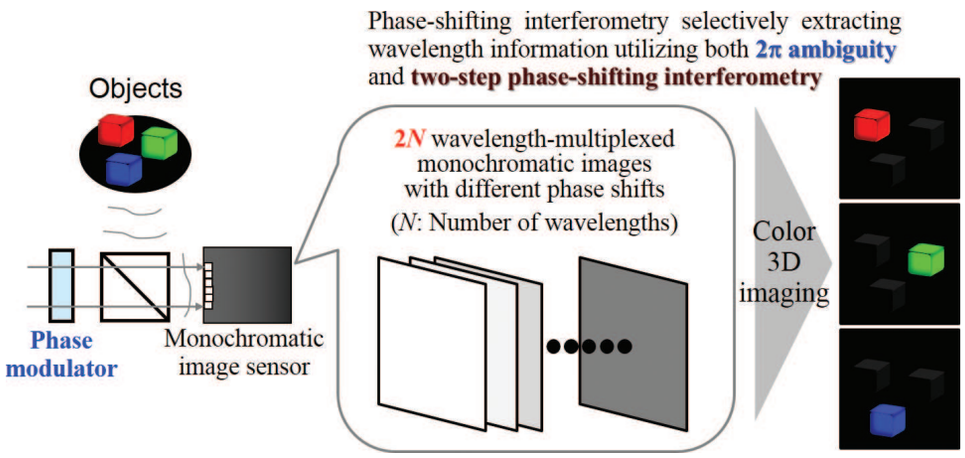


**Figure 8.** Basic concept of 2π-PDM.

The optical setup required for 2π-PDM is the same as that for other PDM techniques. Therefore, the systems in **Figure 4** are applicable to 2π-PDM. In 2π-PDM, various types of two-step phase-shifting methods [52–56] can be employed. When merging Meng's two-step method [53] into 2π-PDM, intensity distributions of reference waves $Ir_{\lambda 1}(x,y) = Ar_{\lambda 1}{}^2(x,y)$ and $Ir_{\lambda 2}(x,y) = Ar_{\lambda 2}{}^2(x,y)$ are sequentially recorded before the measurement by inserting a shutter in the path of the object arm. **Figure 9** describes an algorithm for selectively extracting wavelength information in 2π-PDM adopting Meng's technique. In the case of $N = 2$, a monochromatic image sensor records four wavelength-multiplexed phase-shifted holograms $I(x,y{:}0,0)$, $I(x,y{:}\alpha_1,\text{arb.})$, $I(x,y{:}2\pi M,\alpha_2)$, and $I(x,y{:}-2\pi M,-\alpha_2)$, and intensity distributions of reference waves $Ir_{\lambda 1}(x,y)$ and $Ir_{\lambda 2}(x,y)$. By making use of 2π ambiguity, both a 0th-order diffraction wave $0th_{\lambda 2}(x,y)$ and an intensity distribution of a hologram at an undesired wavelength $I_{\lambda 1}(x,y)$ are removed simultaneously by the subtraction procedure. Therefore, an object wave $U_{\lambda 2}(x,y)$ is extracted from three holograms, although five variables are contained in each hologram. In the case where $\alpha_1$ and $\alpha_2 > 0$, $U_{\lambda 2}(x,y)$ is derived by

$$U_{\lambda 2}(x,y) = [2I(x,y:0,0) - \{I(x,y:2\pi M,\alpha_2) + I(x,y:-2\pi M,-\alpha_2)\}]/\{4Ar_{\lambda 2}(x,y)(1-\cos\alpha_2)\} + j\{I(x,y:2\pi M,\alpha_2) - I(x,y:-2\pi M,-\alpha_2)\}/(4Ar_{\lambda 2}(x,y)\ \sin\alpha_2). \tag{7}$$

From the extracted object wave $U_{\lambda 2}(x,y)$ and the amplitude distribution of the reference wave at $\lambda_2$, the intensity distribution at only $\lambda_2$ component $I_{\lambda 2}(x,y{:}\alpha_2)$ is numerically generated by a computer,

$$I_{\lambda 2\text{cal}}(x,y:\alpha_2) = |U_{\lambda 2}(x,y)|^2 + Ar_{\lambda 2}(x,y)^2 + Ar_{\lambda 2}(x,y)\{U_{\lambda 2}(x,y)\exp(-j\alpha_2) + U_{\lambda 2}{}^*(x,y)\exp(j\alpha_2)\}. \tag{8}$$

If the sum of the intensities of the 0th-order diffraction waves is equal to $|U_{\lambda 1}(x,y)|^2 + Ir_{\lambda 1}(x,y) + |U_{\lambda 2}(x,y)|^2 + Ir_{\lambda 2}(x,y)$, noiseless multiwavelength 3D imaging can be achieved with 2π-PDM adopting Meng's two-step phase-shifting interferometry, according to the procedures described from here. By using the numerically generated images $I_{\lambda 2\text{cal}}(x,y{:}0)$ and $I_{\lambda 2\text{cal}}(x,y{:}\text{arb.})$, intensity distributions at only $\lambda_1$ component $I_{\lambda 1}(x,y{:}0)$ and $I_{\lambda 1}(x,y{:}\alpha_1)$ are obtained from $I(x,y{:}0,0)$ and $I(x,y{:}\alpha_1,\text{arb.})$ as the following expressions:

$$\begin{aligned} I_{\lambda 1}(x,y:0) &= I(x,y:0,0) - I_{\lambda 2\text{cal}}(x,y:0) \\ &= |U_{\lambda 1}(x,y)|^2 + Ar_{\lambda 1}(x,y)^2 + Ar_{\lambda 1}(x,y)\{U_{\lambda 1}(x,y) + U_{\lambda 1}{}^*(x,y)\}, \end{aligned} \tag{9}$$

$$\begin{aligned} I_{\lambda 1}(x,y:\alpha_1) &= I(x,y:\alpha_1,\text{arb.}) - I_{\lambda 2\text{cal}}(x,y:\text{arb.}) \\ &= |U_{\lambda 1}(x,y)|^2 + Ar_{\lambda 1}(x,y)^2 + Ar_{\lambda 1}(x,y)\{U_{\lambda 1}(x,y)\exp(-j\alpha_1) + U_{\lambda 1}{}^*(x,y)\exp(j\alpha_1)\}. \end{aligned} \tag{10}$$

From the obtained $I_{\lambda 1}(x,y{:}0)$ and $I_{\lambda 1}(x,y{:}\alpha_1)$ and amplitude distribution of the reference wave at $\lambda_1$, the object wave at $\lambda_1$ $U_{\lambda 1}(x,y)$ can be analytically extracted by using two-step phase-shifting interferometry.

$$U_{\lambda 1}(x,y) = [\{I_{\lambda 1}(x,y:0) - s(x,y))\} + j\{I_{\lambda 1}(x,y:\alpha_1) - I_{\lambda 1}(x,y:0)\cos\alpha_1 - (1-\cos\alpha_1)s(x,y)\}]/2Ar_{\lambda 1}(x,y), \tag{11}$$

where,

$$s(x,y) = |U_{\lambda 1}(x,y)|^2 + Ar_{\lambda 1}(x,y)^2 = \left(\frac{v-\sqrt{v^2-4uw}}{2u}\right), \tag{12}$$

$$u = 2(1-\cos\alpha_1), \tag{13}$$

$$v = 2\left[(1-\cos\alpha_1)\{I_{\lambda 1}(x,y:0) + I_{\lambda 1}(x,y:\alpha_1)\} + 2Ir_{\lambda 1}(x,y)\sin^2\alpha_1\right], \tag{14}$$

http://dx.doi.org/10.5772/67295

$$w = I_{\lambda 1}(x,y:0)^2 + I_{\lambda 1}(x,y:\alpha_1)^2 - 2I_{\lambda 1}(x,y:0)I_{\lambda 1}(x,y:\alpha_1)\cos\alpha_1 + 2Ir_{\lambda 1}(x,y)^2\sin^2\alpha_1. \quad (15)$$

Thus, the object waves at the desired wavelengths are extracted selectively from four wavelength-multiplexed phase-shifted holograms and intensity distributions of the reference waves. In this way, in the case where the number of wavelengths is $N$, multiwavelength information can be separately extracted from $2N$ holograms. By applying diffraction integrals to the object waves, amplitude and phase distributions of the object on the desired depth are reconstructed at multiple wavelengths. Therefore, a 3D image and wavelength dependency of the object can be obtained simultaneously.

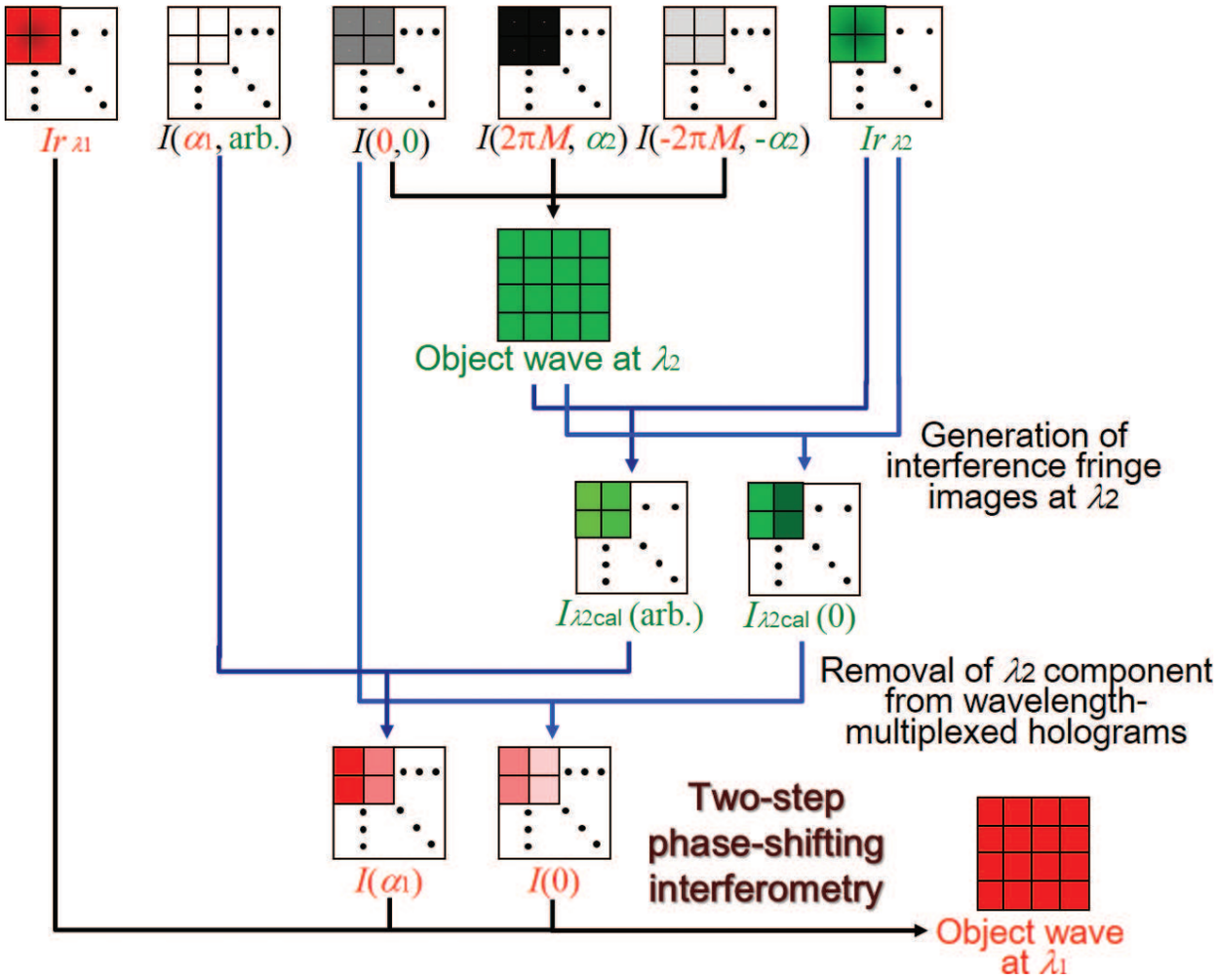


**Figure 9.** Algorithm for selectively extracting wavelength information in 2π-PDM.

Note that an arbitrary phase shift at $\lambda_2$ is allowable in one of the wavelength-multiplexed, phase-shifted, and monochromatic holograms $I(x,y{:}\alpha_1,\text{arb.})$ in a 2π-PDM algorithm described above. Therefore, 2π-PDM conducts asymmetric phase-shifting and belongs to partially generalized phase-shifting interferometry.

## 5. Experimental demonstration of 2π-PDM

We have demonstrated 2π-PDM experimentally to show color 3D imaging ability [38]. **Figure 10** shows a completed model of the optical system illustrated in **Figure 4(a)**. Four wavelength-multiplexed phase-shifted holograms were recorded sequentially by using a mirror with a piezo actuator. Before/after that, two intensity images of two reference waves were sequentially recorded only once. The wavelengths of the lasers were $\lambda_1 = 640$ and $\lambda_2 = 473$ nm. A monochromatic CMOS image sensor was used to record the holograms and reference intensities. The sensor has 12-bit resolution, 2592 × 1944 pixels, and the pixel pitch of 2.2 μm. The mirror with a piezo actuator moved $Z = 0$, 237, and ±320 nm sequentially to generate phase shifts that were required for 2π-PDM. Phase shifts $(\alpha_1,\alpha_2)$ at $(\lambda_1,\lambda_2)$ were (0,0), $(2\pi(\lambda_2/\lambda_1), 2\pi)$, $(2\pi, 2\pi(\lambda_1/\lambda_2))$, and $(-2\pi,-2\pi(\lambda_1/\lambda_2))$. To investigate the phase shifts at their respective wavelengths, interference fringe patterns at the wavelengths were observed before the experimental demonstration, and details were explained in Ref. [38]. Two transparency sheets were set as a color 3D object. The logo of the International Year of Light (IYL) and the characters "2015" were printed on the sheets, and blue and red color films were attached to the logo and characters, respectively. The red "2015" sheet and blue logo sheet were set on the depths of 250 and 320 mm from the image sensor plane, respectively. Opaque sheets were also attached on blue and red color sheets to scatter the object illumination light. Therefore, the 3D color object had a rough surface and scattered object waves illuminated the image sensor. The object wave at the wavelength $\lambda = 473$ nm was extracted from three holograms and the object wave at $\lambda = 640$ nm was obtained by the procedures of Eqs. (7)–(15). For comparison, a colored object image was also reconstructed from a wavelength-multiplexed hologram.

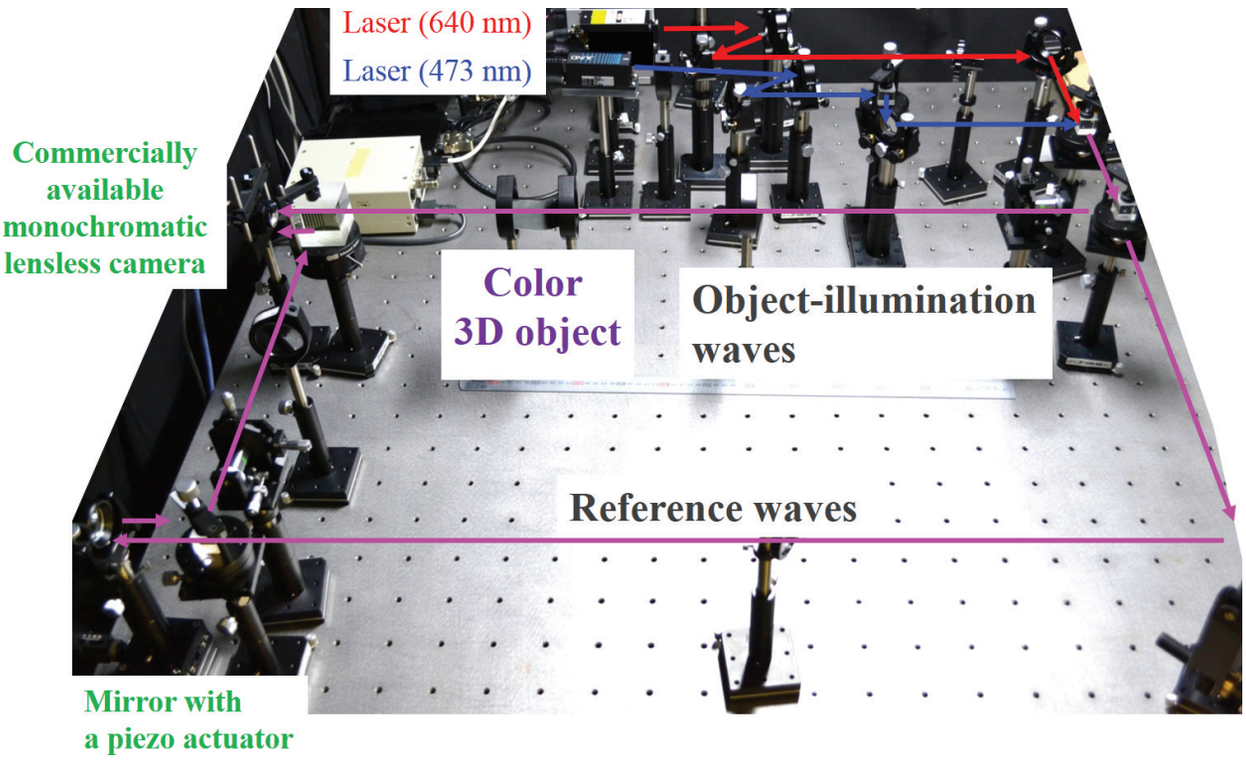


**Figure 10.** Photograph of the constructed dual-wavelength optical system of 2π-PDM.

http://dx.doi.org/10.5772/67295

**Figure 11** shows the experimental results. Wavelength-multiplexed monochromatic images such as **Figure 11(a)** were captured, and wavelength information was superimposed on space and spatial frequency domains as seen in **Figure 11(a)** and **(b)**. **Figure 11(c)** and **(d)** were the images focused digitally at a distance of 320 mm from the image sensor plane and reconstructed by diffraction integral alone and 2π-PDM, respectively. Blue and red color films attached to the sheets absorbed red and blue light, respectively. However, **Figure 11(c)**, which was obtained from a wavelength-multiplexed hologram, indicated the superimpositions of not only the 0th-order diffraction wave and the conjugate image but also image components given by the crosstalk between $I_{\lambda 1}(x,y;\alpha_1)$ and $I_{\lambda 2}(x,y;\alpha_2)$. As a result, color information was not retrieved adequately. In contrast, **Figure 11(d)** showed the removal of the unwanted images, the crosstalk components, and the successful experimental demonstration of clear color imaging by 2π-PDM. **Figure 11(e)** and **(f)** were the object images focused on 250 and 320 mm depths from the sensor plane, which were obtained by an image-reconstruction procedure of 2π-PDM. Thus, we validated 2π-PDM in the imaging of wavelength dependency of absorption for a 3D object and high-quality color 3D imaging ability.

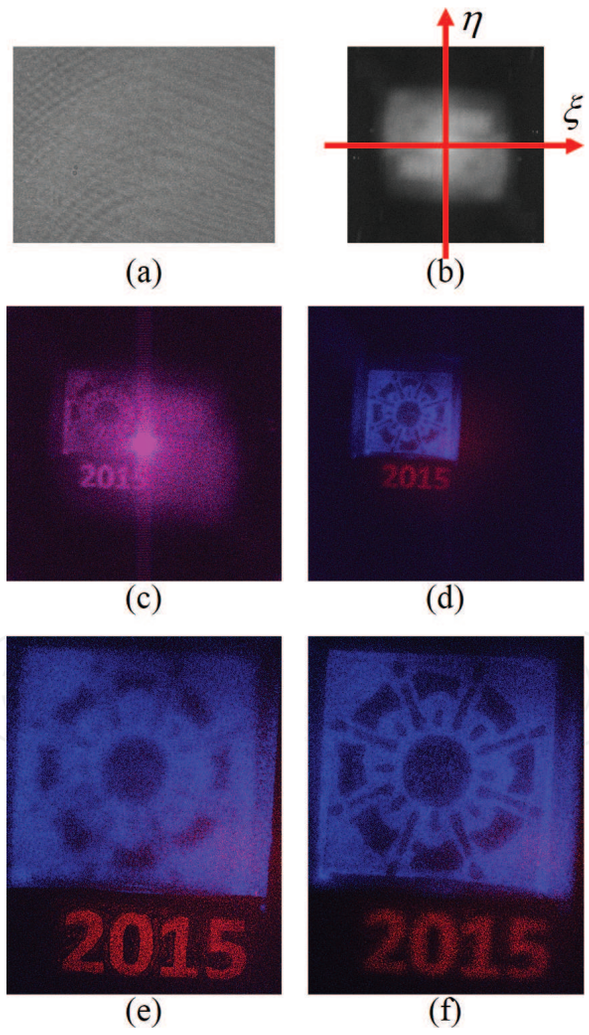


**Figure 11.** Experimental results of 2π-PDM. (a) One of the recorded holograms and (b) its 2D Fourier transformed image. (c) Image reconstructed from the hologram of (a). (d) Whole image reconstructed by 2π-PDM. (c) and (d) are the images digitally focused on 250 mm depth from the image sensor plane. Object images numerically focused on (e) 250 mm and (f) 320 mm depths, which were reconstructed by 2π-PDM.

## 6. Discussions and summary

We have proposed phase-shifting interferometry selectively extracting wavelength information as a novel multiwavelength imaging technique. In this technique, not only multiwavelength images but also the information of 3D space are simultaneously captured by the combination with holography. The technique is characterized as phase-division multiplexing (PDM) of wavelengths, and wavelength information is separately extracted in the space domain from the information of multiple wavelength-multiplexed images. 2π-PDM is the technique to analytically and completely solve the system of equations with $2N$ holograms against $2N + 1$ variables contained in each hologram. An experimental demonstration was conducted and clear color 3D imaging ability was successfully shown. Note that detailed analyses against both the experimental demonstration and the theory in 2π-PDM were reported in Ref. [38].

As future works, constructions of three-color digital holography and multidimensional holography systems are important to realize full-color 3D imaging and multidimensional holographic sensing. **Figure 12** shows an example of the required holograms in three-wavelength 2π-PDM [38] and numerical results for theoretical validation. Phase shifts indicated in **Figure 12(a)** mean that three-color 3D imaging with 2π-PDM is capable, when a spatial light modulator or wave plates are used as phase shifter(s) as described in Ref. [38]. Also, a combination of a piezo and a wave plate or a spatial light modulator will be applicable as another implementation. **Figure 12(b)–(i)** shows the results of a numerical simulation for three-

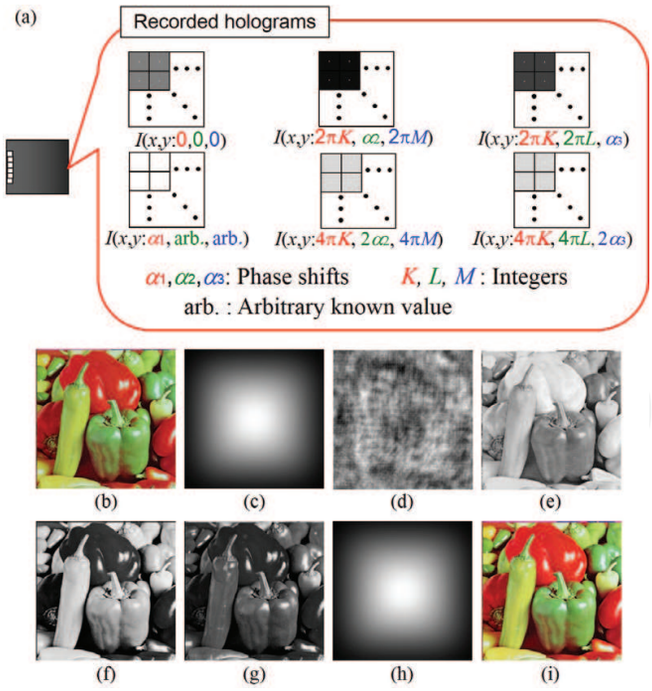


**Figure 12.** (a) An example of holograms required for three-wavelength 2π-PDM and (b)–(i) its numerical results. (b) Amplitude and (c) phase distributions of the assumed object wave and (d) one of three-wavelength-multiplexed phase-shifted holograms. Reconstructed amplitude images at the wavelengths of (e) 640 nm, (f) 532 nm, (g) 473 nm, and (h) phase image at 640 nm. (i) Color synthesized image obtained from (d)–(f). In the results, wave plates are assumed as phase shifters as described in Ref. [38]. The image-reconstruction procedure is in the same manner of dual-wavelength 2π-PDM, which is explained in Section 4.

http://dx.doi.org/10.5772/67295

wavelength 2π-PDM. In this simulation, a three-color object "pepper" with a smooth surface shape, red, green, and blue color wavelengths of 640, 532, and 473 nm, and 200 mm distance between image sensor and object planes, an image sensor with the pixel pitch of 5 μm, 512 × 512 pixels, ideal bit resolution, and $\alpha_1$, $\alpha_2$, $\alpha_3 = \pi/2$ were assumed. These assumptions can be satisfied with the optical system with five quarter wave plates, which is illustrated in Ref. [38]. Numerical results indicate that multiwavelength holographic 3D imaging can be done with high image quality from grayscale wavelength-multiplexed images, if successfully constructed. Improvements on the measurement principle and/or an image-reconstruction algorithm are important to simplify the construction; this is one of the main issues to be solved. From the viewpoint of multidimensional holographic imaging, PDM and 2π-PDM have the potential for not only multiwavelength, but also polarization-imaging digital holography [37] and instantaneous measurement [35], as implementations are described in these references. It is expected that simultaneous imaging of 3D structures, multiple wavelengths, and polarization distribution can be demonstrated with 2π-PDM.

The next step of the PDM techniques is the extension to multicolor holographic 3D image sensing, simultaneous imaging of color and 3D shape with multiwavelength phase unwrapping, dispersion imaging of a 3D specimen, and multidimensional holographic imaging. This technique has prospective applications to multispectral microscopy to observe 3D specimens with a wide field of view, quantitative phase imaging, multicolor lensless 3D camera, multidimensional holographic image sensors, and other multiwavelength 3D imaging applications.

## Acknowledgements

We appreciate Kris Cutsail-Numata for checking the English grammar in this chapter of the book. One of the authors would like to sincerely thank Shu Tahara for encouragement. This research was supported by Japan Science and Technology Agency (JST), PRESTO, Konica Minolta Science and Technology Foundation, The Okawa Foundation, Research Foundation of Tokyo Institute of Technology, the Japan Society for the Promotion of Science (JSPS), MEXT-Supported Program for the Strategic Research Foundation at Private Universities (from 2013 to 2018), and Research Foundation for Opt-Science and Technology.

## Author details

Tatsuki Tahara[1,2*], Reo Otani[3], Yasuhiko Arai[1] and Yasuhiro Takaki[4]

*Address all correspondence to: tahara@kansai-u.ac.jp

1 Faculty of Engineering Science, Kansai University, Suita, Osaka, Japan

2 PRESTO, Japan Science and Technology Agency, Kawaguchi, Saitama, Japan

3 SIGMA KOKI CO., LTD., Hidaka-shi, Saitama, Japan

4 Institute of Engineering, Tokyo University of Agriculture and Technology, Tokyo, Japan

## References


[1] D. Gabor. A new microscopic principle. Nature. 1948;**161**:777–778.

[2] E. N. Leith and J. Upatnieks. Reconstructed wavefronts and communication. J. Opt. Soc. Am. 1962;**52**:1123–1128.

[3] T. Kubota, K. Komai, M. Yamagiwa, and Y. Awatsuji. Moving picture recording and observation of three-dimensional image of femtosecond light pulse propagation. Opt. Express. 2007;**15**:14348–14354.

[4] T. Kubota. 48 years with holography. Opt. Rev. 2014;**21**:883–892.

[5] J. W. Goodman and R. W. Lawrence. Digital image formation from electronically detected holograms. Appl. Phys. Lett. 1967;**11**:77–79.

[6] M. Takeda, H. Ina, and S. Kobayashi. Fourier-transform method of fringe-pattern analysis for computer-based topography and interferometry. J. Opt. Soc. Am. 1982;**72**:156–160.

[7] M. K. Kim, editor. Digital Holographic Microscopy: Principles, Techniques, and Applications. Springer; New York; 2011.

[8] T.-C. Poon and J.-P. Liu, editors. Introduction to Modern Digital Holography with MATLAB. Cambridge University Press; New York; 2014.

[9] Y. Takaki, H. Kawai, and H. Ohzu. Hybrid holographic microscopy free of conjugate and zero-order images. Appl. Opt. 1999;**38**:4990–4996.

[10] V. Mićo, Z. Zalevsky, P. García-Martínez, and J. García. Synthetic aperture superresolution with multiple off-axis holograms. J. Opt. Soc. Am. A. 2006;**23**:3162–3170.

[11] T. Ikeda, G. Popescu, R. R. Dasari, and M. S. Feld. Hilbert phase microscopy for investigating fast dynamics in transparent systems. Opt. Lett. 2005;**30**:1165–1167.

[12] E. Watanabe, T. Hoshiba, and B. Javidi. High-precision microscopic phase imaging without phase unwrapping for cancer cell identification. Opt. Lett. 2013;**38**:1319–1321.

[13] N. Pavillon, K. Fujita, and N. I. Smith. Multimodal label-free microscopy. J. Innov. Opt. Health Sci. 2014;**07**:1330009.

[14] Q. Xian, K. Nitta, O. Matoba, P. Xia, and Y. Awatsuji. Phase and fluorescence imaging by combination of digital holographic microscopy and fluorescence microscopy. Opt. Rev.. 2015;**22**:349–353.

[15] C. Zhang and I. Sato. Image-based separation of reflective and fluorescent components using illumination variant and invariant color. IEEE Trans. Pattern Anal. Mach. Intell. 2013;**35**:2866–2877.

[16] M. Okada, N. I. Smith, A. F. Palonpon, H. Endo, S. Kawata, M. Sodeoka, and K. Fujita. Label-free Raman observation of cytochrome c dynamics during apoptosis. Proc. Natl. Acad. Sci. USA. 2012;**109**:28–32.

[17] Y. Ozeki, W. Umemura, Y. Otsuka, S. Satoh, H. Hashimoto, K. Sumimura, N. Nishizawa, K. Fukui, and K. Itoh. High-speed molecular spectral imaging of tissue with stimulated Raman scattering. Nat. Photon. 2012;**6**:845–851.

[18] N. Tsumura, R. Usuba, K. Takase, T. Nakaguchi, N. Ojima, N. Komeda, and Y. Miyake. Image-based control of skin translucency. Appl. Opt. 2008;**47**:6543–6549.

[19] I. Yamaguchi, T. Matsumura, and J. Kato. Phase-shifting color digital holography. Opt. Lett. 2002;**27**:1108–1110.

[20] J. Kato, I. Yamaguchi, and T. Matsumura. Multicolor digital holography with an achromatic phase shifter. Opt. Lett. 2002;**27**:1403–1405.

[21] C. Yang, A. Wax, I. Georgakoudi, E. B. Hanlon, K. Badizadegan, R. R. Dasari, and M. S. Feld. Interferometric phase-dispersion microscopy. Opt. Lett. 2000;**25**:1526–1528.

[22] Y.-Y. Cheng and J. C. Wyant. Two-wavelength phase shifting interferometry. Appl. Opt. 1984;**23**:4539-4543.

[23] P. Ferraro, S. Grilli, L. Miccio, D. Alfieri, S. D. Nicola, A. Finizio, and B. Javidi. Full color 3-D imaging by digital holography and removal of chromatic aberrations. IEEE J. Disp. Tech. 2008;**4**:97–100.

[24] A. Wada, M. Kato, and Y. Ishii. Large step-height measurements using multiple-wavelength holographic interferometry with tunable laser diodes. J. Opt. Soc. Am. A. 2008;**25**:3013–3020.

[25] P. Xia, Y. Shimozato, Y. Ito, T. Tahara, T. Kakue, Y. Awatsuji, K. Nishio, S. Ura, T. Kubota, and O. Matoba. Improvement of color reproduction in color digital holography by using spectral estimation technique. Appl. Opt. 2011;**50**:H177–H182.

[26] T. Hansel, G. Steinmeyer, R. Grunwald, C. Falldorf, J. Bonitz, C. Kaufmann, V. Kebbel, and U. Griebner. Synthesized femtosecond laser pulse source for two-wavelength contouring with simultaneously recorded digital holograms. Opt. Express. 2009;**17**: 2686–2695.

[27] P. Tankam, Q. Song, M. Karray, J. Li, J. M. Desse, and P. Picart. Real-time three-sensitivity measurements based on three-color digital Fresnel holographic interferometry. Opt. Lett. 2010;**35**:2055–2057.

[28] M. A. Araiza-Esquivel, L. Martínez-León, B. Javidi, P. Andrés, J. Lancis, and E. Tajahuerce. Single-shot color digital holography based on the fractional Talbot effect. Appl. Opt.. 2011;**50**:B96–B101.

[29] P. Gabolde and R. Trebino. Single-shot measurement of the full spatio-temporal field of ultrashort pulses with multi-spectral digital holography. Opt. Express. 2006;**23**:11460–11467.

[30] R. Dändliker, R. Thalmann, and D. Prongué. Two-wavelength laser interferometry using superheterodyne detection. Opt. Lett. 1988;**13**:339–341.

[31] D. Barada, T. Kiire, J. Sugisaka, S. Kawata, and T. Yatagai. Simultaneous two-wavelength Doppler phase-shifting digital holography. Appl. Opt. 2011;**50**:H237–H244.

[32] A. W. Lohmann. Reconstruction of vectorial wavefronts. Appl. Opt. 1965;**4**:1667–1668.

[33] R. Onodera and Y. Ishii. Two-wavelength interferometry that uses a Fourier-transform method. Appl. Opt. 1998;**37**:7988–7994.

[34] T. Tahara, S. Kikunaga, Y. Arai, and Y. Takaki. Phase-shifting interferometry capable of selectively extracting multiple wavelength information and color three-dimensional imaging using a monochromatic image sensor. In: Optics and Photonics Japan 2013 (OPJ); Nov. 13; Nara, Japan. Optical Society of Japan (OSJ); 2013. p. 13aE9 (2 pages). (in Japanese)

[35] T. Tahara, S. Kikunaga, Y. Arai, and Y. Takaki. Phase-shifting interferometry capable of selectively extracting multiple wavelength information and its applications to sequential and parallel phase-shifting digital holography. In: Digital Holography and Three-Dimensional Imaging 2014 (DH), OSA Technical Digest (online); July 14; Seattle, USA. Optical Society of America (OSA); 2014. p. DM3B.4 (3 pages).

[36] T. Tahara, R. Mori, S. Kikunaga, Y. Arai, and Y. Takaki . Dual-wavelength phase-shifting digital holography selectively extracting wavelength information from wavelength-multiplexed holograms. Opt. Lett. 2015;**40**:2810–2813.

[37] T. Tahara, S. Kikunaga, Y. Arai. Digital holography apparatus and digital holography method. Application number PCT/JP2014/067556. Filing date July 1, 2014.

[38] T. Tahara, R. Mori, Y. Arai, and Y. Takaki. Four-step phase-shifting digital holography simultaneously sensing dual-wavelength information using a monochromatic image sensor. J. Opt. (IOP Publishing). 2015;**17**(12):125707 (10 pages).

[39] T. Tahara, R. Otani, Y. Arai, and Y. Takaki. Multiwavelength digital holography based on phase-division multiplexing using arbitrary symmetric phase shifts. In: Digital Holography and Three-Dimensional Imaging 2016 (DH), OSA Technical Digest (online); July 27; Heidelberg, USA. Optical Society of America (OSA); 2016. p. DW5E.2 (3 pages).

[40] J. H. Bruning, D. R. Herriott, J. E. Gallagher, D. P. Rosenfeld, A. D. White, and D. J. Brangaccio. Digital wavefront measuring interferometer for testing optical surfaces and lenses. Appl. Opt. 1974;**13**:2693–2703.

[41] Y. Ishii and R. Onodera. Two-wavelength laser-diode interferometry that uses phase-shifting techniques. Opt. Lett. 1991;**16**:1523–1525.

[42] R. Onodera and Y. Ishii. Two-wavelength phase-shifting interferometry insensitive to the intensity modulation of dual laser diodes. Appl. Opt. 1994;**33**:5052–5061.

[43] I. Yamaguchi and T. Zhang. Phase-shifting digital holography. Opt. Lett. 1997;**31**:1268–1270.

[44] S. Tamano, Y. Hayasaki, and N. Nishida. Phase-shifting digital holography with a low-coherence light source for reconstruction of a digital relief object hidden behind a light-scattering medium. Appl. Opt. 2006;**45**:953–959.

[45] A. Stern and B. Javidi. Improved-resolution digital holography using the generalized sampling theorem for locally band-limited fields. J. Opt. Soc. Am. A. 2006;**23**:1227–1235.

[46] J. Rosen and G. Brooker. Non-scanning motionless fluorescence three-dimensional holographic microscopy. Nat. Photon. 2008;**2**:190–195.

[47] D. Naik, T. Ezawa, Y. Miyamoto, and M. Takeda. Phase-shift coherence holography. Opt. Lett. 2010;**35**:1728–1730.

[48] Y.-C. Lin, C.-J. Cheng, and T.-C. Poon. Optical sectioning with a low-coherence phase-shifting digital holographic microscope. Appl. Opt. 2011;**50**:B25–B30.

[49] Y. Lim, S.-Y. Lee, and B. Lee. Transflective digital holographic microscopy and its use for probing plasmonic light beaming. Opt. Express. 2011;**19**:5202–5212.

[50] R. Horisaki and T. Tahara. Phase-shift binary digital holography. Opt. Lett. 2014;**39**:6375–6378.

[51] W. Li, C. Shi, M. Piao, and N. Kim. Multiple-3D-object secure information system based on phase shifting method and single interference. Appl. Opt. 2016;**55**:4052–4059.

[52] S. Almazán-Cuellar and D. Maracala-Hernandez. Two-step phase-shifting algorithm. Opt. Eng. 2003;**42**:3524–3531.

[53] X. F. Meng, L. Z. Cai, X. F. Xu, X. L. Yang, X. X. Shen, G. Y. Dong, and Y. R. Wang. Two-step phase-shifting interferometry and its application in image encryption. Opt. Lett. 2006;**31**:1414–1416.

[54] T. Kiire, S. Nakadate, and M. Shibuya. Digital holography with a quadrature phase-shifting interferometer. Appl. Opt. 2009;**48**:1308–1315.

[55] J. -P. Liu and T.-C. Poon. Two-step-only quadrature phase-shifting digital holography. Opt. Lett. 2009;**34**:250–252.

[56] J. Vargas, J. Antonio Quiroga, T. Belenguer, M. Servín, and J. C. Estrada. Two-step self-tuning phase-shifting interferometry. Opt. Express. 2011;**19**:638–648.

IntechOpen